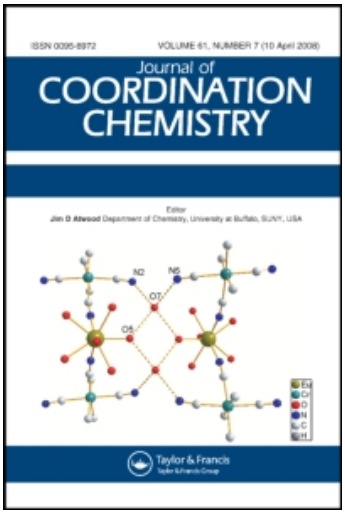

Journal of Coordination Chemistry
Publication details, including instructions for authors and subscription information:
http://www.informaworld.com/smpp/title~content=t713455674

Two-dimensional layer polyoxometalate-based inorganic metal-organic hybrid supramolecular networks woven by Cu ··· $O_{polyoxoanion}$ short contact weak interactions

Cai-Ming Liu[a]; Jian-Ying Zhang[a]; De-Qing Zhang[a]
[a] Beijing National Laboratory for Molecular Sciences, Center for Molecular Science, Institute of Chemistry, Chinese Academy of Sciences, Beijing 100080, P. R. China

First published on: 23 July 2007

To cite this Article Liu, Cai-Ming , Zhang, Jian-Ying and Zhang, De-Qing(2008) 'Two-dimensional layer polyoxometalate-based inorganic metal-organic hybrid supramolecular networks woven by Cu ··· $O_{polyoxoanion}$ short contact weak interactions', Journal of Coordination Chemistry, 61: 4, 627 — 639, First published on: 23 July 2007 (iFirst)
To link to this Article: DOI: 10.1080/00958970701369791
URL: http://dx.doi.org/10.1080/00958970701369791

Journal of Coordination Chemistry
Vol. 61, No. 4, 20 February 2008, 627–639

Taylor & Francis
Taylor & Francis Group

Two-dimensional layer polyoxometalate-based inorganic metal–organic hybrid supramolecular networks woven by $Cu\cdots O_{polyoxoanion}$ short contact weak interactions

CAI-MING LIU*, JIAN-YING ZHANG and DE-QING ZHANG

Beijing National Laboratory for Molecular Sciences, Center for Molecular Science, Institute of Chemistry, Chinese Academy of Sciences, Beijing 100080, P. R. China

(*Received 11 December 2006; in final form 29 January 2007*)

Two polyoxometalate-based inorganic metal-organic hybrid supramolecular complexes $[Cu(2,2'\text{-bpy})_2]_2[V^{IV}{}_2Mo^{V}{}_5Mo^{VI}{}_7O_{38}(PO_4)]$ (**1**) (2,2′-bpy = 2,2′-bipyridine) and $[Cu(2,2'\text{-bpy})_2]_2[Mo^{V}Mo^{VI}{}_{11}O_{36}(PO_4)]\cdot 3H_2O$ (**2**), have been hydrothermally prepared and structurally characterized by single-crystal X-ray diffraction. Both complexes are constructed from polyoxoanions (the bivanadyl capped α-Keggin polymolybdate anion $[V^{IV}{}_2Mo^{V}{}_5Mo^{VI}{}_7O_{38}(PO_4)]^{4-}$ for **1** and the reduced 12-molybdophosphate anion $[Mo^{V}Mo^{VI}{}_{11}O_{36}(PO_4)]^{4-}$ for **2**) and copper(II) complex cations $[Cu(2,2'\text{-bpy})_2]^{2+}$, forming two-dimensional (2D) layer network structures, in which the polyoxoanion and the complex fragment cation connect with each other through $Cu\cdots O_{polyoxoanion}$ short contact weak interactions, which mediate ferromagnetic interaction.

Keywords: Polyoxometalate; Hybrid material; Crystal structure; Weak interaction; Copper(II) complex; Magnetic property

1. Introduction

The target of crystal engineering is to master collective crystal properties by controlling the manner that molecular building blocks are assembled in the desired (designed) superstructure [1]. Therefore, the synthesis and/or identification of feasible molecular building blocks and understanding how they are combined in a directed way by self-assembly are of paramount importance in solid-state chemistry and crystal engineering [1].

Polyoxometalates have become extremely versatile building blocks for the construction of the functionally active inorganic metal-organic hybrid solid materials owing to their diversity of charges, shapes and sizes [2]. Furthermore, coordination ability of polyoxometalates make the architecture of abundant extended structures possible: these polyoxometalates act as special ligands to bond one or more metal ions,

*Corresponding author. Email: cmliu@iccas.ac.cn

Journal of Coordination Chemistry
ISSN 0095-8972 print/ISSN 1029-0389 online © 2008 Taylor & Francis
DOI: 10.1080/00958970701369791

generating polyoxoanion–supported or bridged inorganic metal-organic hybrid solid materials, including discrete clusters [3], one-dimensional (1D) chains [4], two-dimensional (2D) networks [5] and three-dimensional (3D) frameworks [6]. Less attention has been paid to assembly of polyoxometalate-based inorganic metal-organic hybrid supramolecular structures although non-covalent weak interactions have been widely studied in supramolecular coordination chemistry [8, 9]. For examples, hydrogen bonds and π–π stacking interactions play important roles in self-assembly, molecular recognition processes and crystal engineering [7]; the Ag $\cdots$ Ag short contact weak interaction had been utilized to construct many extended coordination polymer structures [8]; and the $Ag\cdots O_{nitrate}$ short contact weak interaction can guide $\{[Ag(4\text{-pytz})]NO_3\}_\infty$ [4-pytz = 3,6-di(pyridin-4-yl)-1,2,4,5-tetrazine] [9] to form a 3D helical staircase supramolecular structure rather than 1D linear chain structures of $\{[Ag(4\text{-pytz})]PF_6\}_\infty$ and $\{[Ag(4\text{-pytz})]BF_4\}_\infty$ [9].

Several polyoxometalate-based inorganic metal-organic hybrid supramolecular complexes were constructed through hydrogen bonds between polyoxoanion and transition metal complex fragment cations [10], and $Ni\cdots O_{polyoxoanion}$ short contact weak interaction was observed in our recently reported polyoxometalate-based inorganic metal-organic hybrid supramolecular complex $\{[Mo^{VI}{}_5Mo^{V}{}_3V^{IV}{}_8O_{40}(PO_4)][Ni(en)_2]\}[Ni(en)_2]_2\cdot 4H_2O$ (en = ethylenediamine) [4g], where each $[Mo^{VI}{}_5Mo^{V}{}_3V^{IV}{}_8O_{40}(PO_4)]^{6-}$ cluster in $\{[Mo^{VI}{}_5Mo^{V}{}_3V^{IV}{}_8O_{40}(PO_4)][Ni(en)_2]\}^{4-}$ anion chain connects with two discrete cations $[Ni(en)_2]^{2+}$ through the inter-molecular Ni $\cdots$ O short contacts to form a sandwich-like chain structure. It is of interest to investigate whether or not direct, short contact weak interaction between terminal oxygen in polyoxoanion and the transition metal center in complex cation can be exploited to maintain high-dimensional polyoxometalate-based inorganic metal-organic hybrid supramolecular networks. Herein we report two 2D polyoxometalate-based inorganic metal-organic hybrid layer supramolecular complexes $[Cu(2,2'\text{-bpy})_2]_2[V^{IV}{}_2Mo^{V}{}_5Mo^{VI}{}_7O_{38}(PO_4)]$ (**1**) (2,2′-bpy = 2,2′-bipyridine) and $[Cu(2,2'\text{-bpy})_2]_2[Mo^{V}Mo^{VI}{}_{11}O_{36}(PO_4)]\cdot 3H_2O$ (**2**), where the $Cu\cdots O_{polyoxoanion}$ short contact weak interactions between the polyoxoanions and the complex fragment cations $[Cu(2,2'\text{-bpy})_2]^{2+}$ extend both structures into 2D layer supramolecular arrays.

2. Experimental

2.1. *Materials and methods*

$H_3[P(Mo_3O_{10})_4]\cdot xH_2O$ (with a reference FW of 1825.25) was obtained from Strem Chemicals, Inc. All other chemicals were of reagent grade and purchased from Beijing Shuanghuan Chemicals, Inc. Elemental analyses (C, H and N) were performed on a Heraeus CHN-Rapid elemental analyzer. The infrared spectra were recorded on a Pekin-Elmer 2000 spectrophotometer using pressed KBr pallets. The magnetic susceptibility measurements were carried out on polycrystalline samples (31.42 mg of **1** and 18.14 mg of **2**) using a Quantum Design MPMS-XL5 SQUID magnetometer, in the temperature range 2–300 K and at applied field of 0.2T. Diamagnetic corrections were estimated from Pascal's constants for all constituent atoms.

2.2. *Preparation of 1*

A mixture of NH_4VO_3 (3.0 mmol), $H_3[P(Mo_3O_{10})_4]\cdot xH_2O$ (0.5 mmol), $Cu(CH_3CO_2)_2\cdot H_2O$ (1.0 mmol), 2,2′-bipyridine (2.0 mmol) and H_2O (14 mL) was stirred for 20 min. The mixture was then transferred to a Teflon-lined stainless steel autoclave (23 mL) and kept at 160°C for 10 days. After the autoclave had cooled to room temperature over 6–7 h, black block-shaped crystals of **1** were isolated from blue mother liquid and washed with water, then dried at ambient temperature. Yield 45% based on copper. Anal. Calcd for $C_{40}H_{32}Cu_2Mo_{12}N_8O_{42}PV_2$ **1**: C, 17.74; H, 1.19; N, 4.14%; Found: C, 17.69; H, 1.24; N, 4.11%. IR (KBr, cm^{-1}): 2925(w), 1632(w), 1602(m), 1570(w), 1494(w), 1471(w), 1441(s), 1314(w), 1250(w), 1215(w), 1169(w), 1047(w), 964(s), 935(vs), 899(m), 792(s), 763(vs), 731(m).

2.3. *Preparation of 2*

A mixture of NH_4VO_3 (3.0 mmol), $H_3[P(Mo_3O_{10})_4]\cdot xH_2O$ (0.5 mmol), $Cu(NO_3)_2\cdot 6H_2O$ (1.0 mmol), 2,2′-bipyridine (2.0 mmol), $H_2C_2O_4$ (1.0 mmol) and H_2O (10 mL) was stirred for 20 min. The mixture was then transferred to a Teflon-lined stainless steel autoclave (23 mL) and kept at 170°C for 7 days. After the autoclave had cooled to room temperature overnight, black block-shaped crystals of **2** were isolated, washed with water and dried at ambient temperature. Yield 75% based on copper. Anal. Calcd for $C_{40}H_{38}Cu_2Mo_{12}N_8O_{43}P$ **2**: C, 18.28; H, 1.46; N, 4.26%; Found: C, 18.25; H, 1.51; N, 4.22%. IR (KBr, cm^{-1}): 3448(br, s), 3078(w), 1604(w), 1496(w), 1473(w), 1444(m), 1316(w), 1251(w), 1167(w), 1058(m), 949(s), 872(s), 798(vs), 728(m).

2.4. *X-ray crystal structure determination*

Suitable single crystals of **1** (with dimensions $0.57\times0.36\times0.24\,mm^3$) and **2** (with dimensions $0.51\times0.26\times0.21\,mm^3$) were mounted on a Rigaku RAXIS RAPID IP imaging plate system with Mo-Kα radiation ($\lambda=0.71073$ Å) at 293(2) K. A total of 58984 reflections were collected in the range $2.23^\circ<\theta<27.46^\circ$ ($-23\le h\le23$, $-22\le k\le22$, $-26\le l\le26$), of which 7255 are unique ($R_{int}=0.0418$) and 3845 with $I>2\sigma(I)$ were used in the refinement of the structure of **1**. For the structure of **2**; a total of 60999 reflections were collected in the range $2.38^\circ<\theta<27.48^\circ$ ($-23\le h\le23$, $-22\le k\le22$, $-26\le l\le26$), of which 7317 are unique ($R_{int}=0.0694$) and 5497 with $I>2\sigma(I)$ were used in the refinement. Empirical absorption corrections from Ψ scan were applied. Both structures were solved by direct methods and refined by a full matrix least-squares technique based on F^2 using SHELXL 97. All non-hydrogen atoms were refined anisotropically, and all hydrogen atoms except those in solvent water molecules of **2** were allowed for as riding atoms. Selected crystallographic data and structure determination parameters for **1** and **2** are given in table 1. Selected bond lengths and angles for **1** and **2** are listed in tables 2 and 3, respectively.

Table 1. Crystal data for **1** and **2**.

	1	**2**
Formula	$C_{40}H_{32}Cu_2Mo_{12}N_8O_{42}PV_2$	$C_{40}H_{38}Cu_2Mo_{12}N_8O_{43}P$
Formula weight	2707.95	2628.11
T (K)	293(2)	293(2)
Crystal system	Orthorhombic	Orthorhombic
Space group	*Pbca*	*Pbca*
a (Å)	18.271(4)	18.186(4)
b (Å)	17.051(3)	17.136(3)
c (Å)	20.634(4)	20.553(4)
V (Å^3)	6428(2)	6405(2)
Z	4	4
D_c (g cm^{-3})	2.798	2.719
μ(Mo-Kα) (mm^{-1})	3.309	3.048
Reflections collected	58984	60999
Independent reflections	7255 [$R_{(int)} = 0.0418$]	7317 [$R_{(int)} = 0.0694$]
Observed data [$I > 2\sigma(I)$]	3845	5497
Final R_1[a], wR_2[b] [$I > 2\sigma(I)$]	0.0456, 0.1022	0.0458, 0.1232
Goodness-of-fit on F^2	0.813	0.979

[a]$R_1 = \sum||F_o| - |F_c||/\sum|F_o|$, [b]$wR_2 = \sum\{[w(F_o^2 - F_c^2)^2]/\sum[wF_o^2]^2\}^{1/2}$.

Table 2. Bond lengths (Å) and angles (°) for **1**.[a]

Cu(1)–N(3)	1.971(6)	Cu(1)–N(1)	1.980(6)
Cu(1)–N(4)	1.982(6)	Cu(1)–N(2)	1.982(6)
V(1)–O(5)	1.613(6)	V(1)–O(12)	1.896(6)
V(1)–O(23)	1.917(6)	V(1)–O(22)	1.901(6)
V(1)–O(18)	1.919(6)	Mo(1)–O(16)	1.641(5)
Mo(1)–O(6)	1.778(6)	Mo(1)–O(7)	1.815(6)
Mo(1)–O(23)	1.991(5)	Mo(1)–O(12)	2.048(6)
Mo(2)–O(13)	1.631(5)	Mo(2)–O(8)	1.821(6)
Mo(2)–O(11)	1.850(6)	Mo(2)–O(18)	1.960(5)
Mo(2)–O(23)	1.996(5)	Mo(3)–O(20)	1.640(5)
Mo(3)–O(19)	1.802(5)	Mo(3)–O(10)	1.821(6)
Mo(3)–O(18)	1.999(5)	Mo(3)–O(22)	2.027(5)
Mo(4)–O(14)	1.648(5)	Mo(4)–O(15)	1.840(6)
Mo(4)–O(17)	1.848(6)	Mo(4)–O(12)	1.988(6)
Mo(4)–O(22)	1.972(5)	Mo(5)–O(21)	1.632(5)
Mo(5)–O(17)#1	1.854(6)	Mo(5)–O(8)	1.862(6)
Mo(5)–O(19)	1.920(6)	Mo(5)–O(7)#1	1.926(6)
Mo(6)–O(9)	1.616(5)	Mo(6)–O(11)#1	1.848(6)
Mo(6)–O(15)	1.857(6)	Mo(6)–O(10)	1.922(6)
Mo(6)–O(6)#1	1.956(5)		
N(3)–Cu(1)–N(1)	101.9(3)	N(3)–Cu(1)–N(4)	82.2(3)
N(1)–Cu(1)–N(4)	157.2(3)	N(3)–Cu(1)–N(2)	150.3(3)
N(1)–Cu(1)–N(2)	82.6(3)	N(4)–Cu(1)–N(2)	105.1(3)

[a]Symmetry code: (#1) $-x, -y+2, -z+1$.

3. Results and discussion

3.1. *Syntheses*

Hydrothermal techniques are an effective approach to preparation of inorganic metal-organic hybrid polyoxometalates with diverse architectures [3a, 3b, 3d–3m, 4, 5a–5f, 5h–5l, 6], especially for those with metals in high oxidation states because the

Table 3. Bond lengths (Å) and angles (°) for **2**.[b]

Cu(1)–N(2)	1.962(5)	Cu(1)–N(4)	1.968(5)
Cu(1)–N(3)	1.971(5)	Cu(1)–N(1)	1.989(5)
Mo(1)–O(16)	1.640(4)	Mo(1)–O(5)	1.841(5)
Mo(1)–O(17)	1.865(5)	Mo(1)–O(18)	1.913(5)
Mo(1)–O(14)	1.937(5)	Mo(2)–O(13)	1.648(4)
Mo(2)–O(22)	1.823(5)	Mo(2)–O(12)#1	1.846(5)
Mo(2)–O(21)	1.945(4)	Mo(2)–O(20)	1.954(5)
Mo(3)–O(19)	1.660(4)	Mo(3)–O(20)	1.841(5)
Mo(3)–O(18)	1.844(5)	Mo(3)–O(10)#1	1.922(5)
Mo(3)–O(15)	1.975(5)	Mo(4)–O(9)	1.643(4)
Mo(4)–O(21)	1.836(4)	Mo(4)–O(14)	1.841(5)
Mo(4)–O(7)#1	1.946(5)	Mo(4)–O(8)	1.976(5)
Mo(5)–O(11)	1.652(4)	Mo(5)–O(8)	1.812(5)
Mo(5)–O(10)	1.852(5)	Mo(5)–O(17)	1.936(5)
Mo(5)–O(22)#1	1.989(5)	Mo(6)–O(6)	1.638(4)
Mo(6)–O(15)	1.812(4)	Mo(6)–O(7)	1.829(5)
Mo(6)–O(5)	1.945(4)	Mo(6)–O(12)	1.969(5)
N(2)–Cu(1)–N(4)	101.7(2)	N(2)–Cu(1)–N(3)	158.1(2)
N(4)–Cu(1)–N(3)	83.0(2)	N(2)–Cu(1)–N(1)	83.1(2)
N(4)–Cu(1)–N(1)	148.8(2)	N(3)–Cu(1)–N(1)	104.2(2)

[b]Symmetry code: (#1) $-x, -y, -z$.

organonitrogen species used act not only as ligands, but also as reducing agents under hydrothermal conditions. The oxidation states of all vanadium atoms and part of molybdenum atoms in **1** and one molybdenum atom in **2** were reduced ($V^{V} \rightarrow V^{IV}$ and $Mo^{VI} \rightarrow Mo^{V}$) during hydrothermal reaction processes. Complex **2** containing $[Mo^{V}Mo^{VI}{}_{11}O_{36}(PO_4)]^{4-}$ suggests the existence of oxalic acid in starting materials for **2** probably prevents formation of mixed molybdenum–vanadium heteropolyoxometalate.

3.2. *Crystal structures*

The structure of **1** consists of discrete bivanadyl capped α-Keggin polymolybdate anion $[V^{IV}{}_2Mo^{V}{}_5Mo^{VI}{}_7O_{38}(PO_4)]^{4-}$ and copper(II) complex fragment cation $[Cu(2,2'\text{-bpy})_2]^{2+}$(figure 1). The reduced mixed molybdenum-vanadium heteropolyoxoanion $[V^{IV}{}_2Mo^{V}{}_5Mo^{VI}{}_7O_{38}(PO_4)]^{4-}$ can be described as an α-Keggin core structure of $[Mo_{12}O_{36}(PO_4)]^{8-}$ capped by two additional five coordinate terminal $[VO]^{2+}$ units, and a disordered PO_4^{3-} anion is located in the center of the polyoxoanion as a guest. This bicapped α-Keggin structure is very similar to those in $(Et_3NH)_5[PMo^{V}{}_6Mo^{VI}{}_6O_{40}(V^{IV}O)_2]$ (Et_3N = triethylamine) [11], and $[V^{IV}{}_2Mo^{V}{}_5Mo^{VI}{}_7O_{38}(PO_4)][Cu^{I}{}_6(2,3'\text{-bipy})_6(2,3'\text{-bipy-O})_2]$ [4i], but the polyoxoanion $[V^{IV}{}_2Mo^{V}{}_5Mo^{VI}{}_7O_{38}(PO_4)]^{4-}$ in $[V^{IV}{}_2Mo^{V}{}_5Mo^{VI}{}_7O_{38}(PO_4)][Cu^{I}{}_6(2,3'\text{-bipy})_6(2,3'\text{-bipy-O})_2]$ [4i] is a special ligand to covalently bridge trinuclear copper(I) complex fragments $[Cu^{I}{}_3(2,3'\text{-bipy})_3(2,3'\text{-bipy-O})]^{2+}$, forming a 1D extended ribbon structure. The Mo–O and V–O bond lengths in **1** are Mo–O_t, 1.616(5)–1.648(5) Å; Mo–O_b, 1.778(6)–2.048(6) Å; V–O_t, 1.613(6) Å and V–O_b, 1.896(6)–1.919(6) Å.

The copper(II) in the complex fragment cation $[Cu(2,2'\text{-bpy})_2]^{2+}$ is coordinated by two 2,2′-bipy ligands to generate a distorted $[CuN_4]$ tetrahedral geometry, which is quite similar to those in $[Cu(2,2'\text{-bpy})_2]X_2\{X = BF_4^-$ [12a], ClO_4^- [12b] and PF_6^- [12c]} and

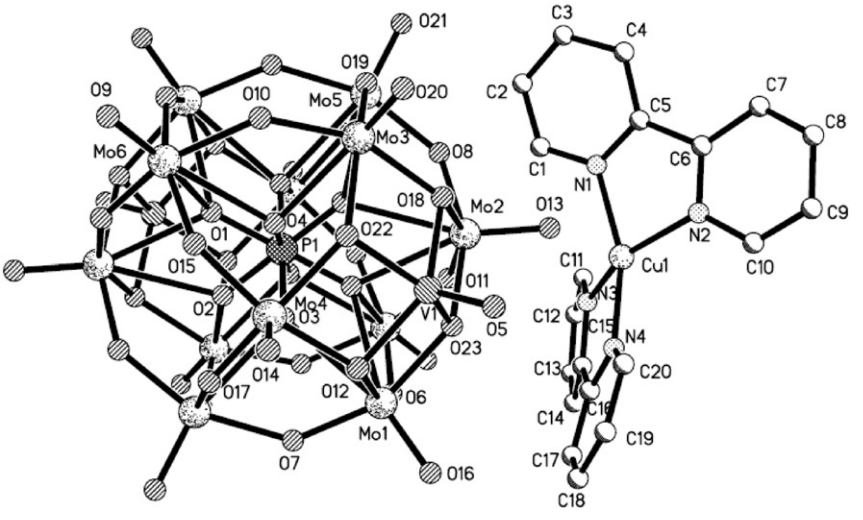

Figure 1. Molecular drawing of **1** with atom labels; all H atoms are omitted for clarity.

$\{[Cu(bppn)](ClO_4)_2\}_2 \cdot H_2O$ [bppn = *N*, *N*′-propylenebis(2-benzoylpyridneiminato)] [13]. The Cu–N bond distances of 1.971(6)–1.982(6) Å (average 1.979 Å) are comparable with those in $[Cu(2,2'\text{-bpy})_2](BF_4)_2$ (average 1.990 Å) [12a], $[Cu(2,2'\text{-bpy})_2](ClO_4)_2$ (average 1.997 Å) [12b], $[Cu(2,2'\text{-bpy})_2](PF_6)_2$ (average 1.958 Å) [12c] and $\{[Cu(bppn)](ClO_4)_2\}_2 \cdot H_2O$ (average 1.989 and 1.984 Å) [13].

The most unusual structural feature of **1** is that a 2D supramolecular network is formed (figure 2). There exist inter-molecular Cu···O short contact weak interactions between discrete complex fragment cations $[Cu(2,2'\text{-bpy})_2]^{2+}$ and heteropolyoxoanion $[V^{IV}{}_2Mo^{V}{}_5Mo^{VI}{}_7O_{38}(PO_4)]^{4-}$ with Cu···O distances of 2.560 and 2.864 Å. Each $[V^{IV}{}_2Mo^{V}{}_5Mo^{VI}{}_7O_{38}(PO_4)]^{4-}$ cluster connects with two cations $[Cu(2,2'\text{-bpy})_2]^{2+}$, consequently, a 2D supramolecular layer is formed in the *ac*-plane. To our knowledge, complex **1** is the first 2D mixed molybdenum–vanadium polyoxometalate-based inorganic metal-organic hybrid layer supramolecular complex constructed through short contact weak interactions between the terminal oxygen in polyoxoanions and a transition metal center in complex fragment cations, although the intermolecular Ni···O weak contact interactions were observed in another 1D chain complex $\{[Mo^{VI}{}_5Mo^{V}{}_3V^{IV}{}_8O_{40}(PO_4)][Ni(en)_2]\}[Ni(en)_2]_2 \cdot 4H_2O$ [4g], and the metal···anion oxygen short contact weak interaction had also been observed to play important role in the construction of coordination polymer supramolecular structures [8, 9].

Assignment of the oxidation states for Mo and V agree with the electric charge and bond valence sum calculations [14]. Using an empirical bond valence calculation, $S = \exp[1 - (R - R_0)/B]$ (S = bond valence, R = bond length), the valence sums for twelve Mo atoms are Mo1(2×): 5.488, Mo2(2×): 5.489, Mo3(2×): 5.393, Mo4(2×): 5.442, Mo5(2×): 5.449, Mo6(2×): 5.588, the average value of which is 5.48 (the expected average value for $Mo^{V}{}_5Mo^{VI}{}_7$ is 5.58); and for two V atoms are V1(2×): 4.192. The calculated results suggest that both V centers are in the +4 oxidation state, while five Mo centers are in the +5 oxidation state with five delocalized electrons. Similar mixed-valence Mo atoms have also been found in other mixed molybdenum-vanadium heteropolyoxometalates [3g–3i, 3k–3m, 4f, 4g, 4i, 5i].

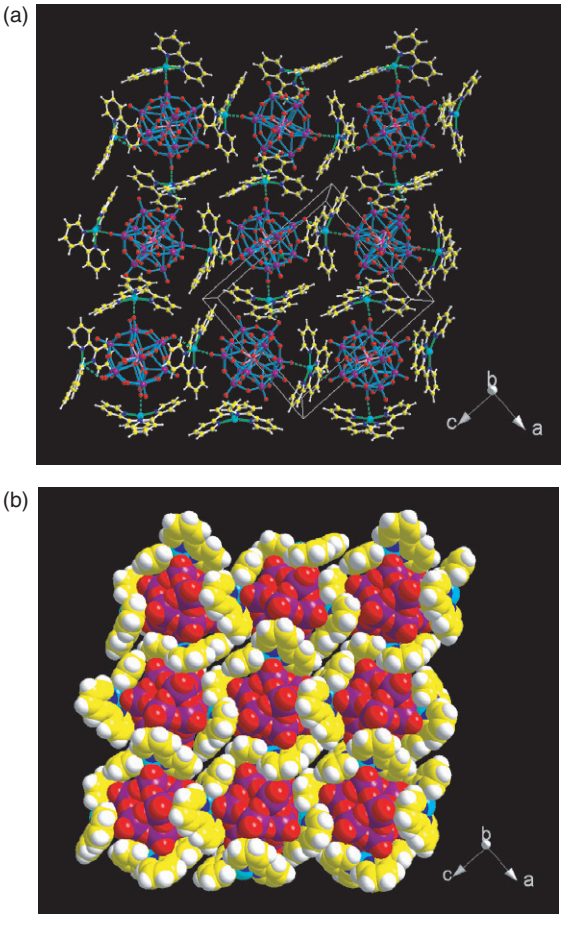

Figure 2. (a) A view of the 2D supramolecular layer network of **1** constructed from the polyoxoanion $[V^{IV}{}_2Mo^{V}{}_5Mo^{VI}{}_7O_{38}(PO_4)]^{4-}$ and the copper(II) complex fragment cation $[Cu(2,2'\text{-bpy})_2]^{2+}$ linked by $Cu\cdots O_{polyoxoanion}$ short contact weak interactions, all H atoms are omitted for clarity. (b) Space-filling model for **1** showing each polyoxoanion is surrounded by four cations.

The structure of **2** is composed of discrete reduced 12-molybdophosphate anions $[Mo^{V}Mo^{VI}{}_{11}O_{36}(PO_4)]^{4-}$, copper(II) complex fragment cations $[Cu(2,2'\text{-bpy})_2]^{2+}$ and crystalline water (figure 3). One difference from the starting material $H_3[P(Mo_3O_{10})_4]\cdot xH_2O$ is the valence value of one molybdenum atom in the α-Keggin anion $[Mo^{V}Mo^{VI}{}_{11}O_{36}(PO_4)]^{4-}$ of **2** was reduced from +6 into +5. Similar to **1**, the coordination sphere of the copper(II) site in the complex fragment cation $[Cu(2,2'\text{-bpy})_2]^{2+}$ of **2** is defined by four nitrogen atoms from two 2,2′-bipy ligands, exhibiting a distorted $[CuN_4]$ tetrahedral configuration. The Cu(II)–N bond distances of 1.962(5)–1.989(5) Å (average 1.973 Å) are very close to those in **1** (average 1.979 Å).

Between the discrete complex fragment cation $[Cu(2,2'\text{-bpy})_2]^{2+}$ and the polyoxoanion $[Mo^{V}Mo^{VI}{}_{11}O_{36}(PO_4)]^{4-}$, intermolecular $Cu\cdots O$ short contact weak interactions, instead of Cu–O covalent bonds, extend the structure into a 2D layer supramolecular array in the *ac*-plane (figure 4), the $Cu\cdots O$ distances of 2.578

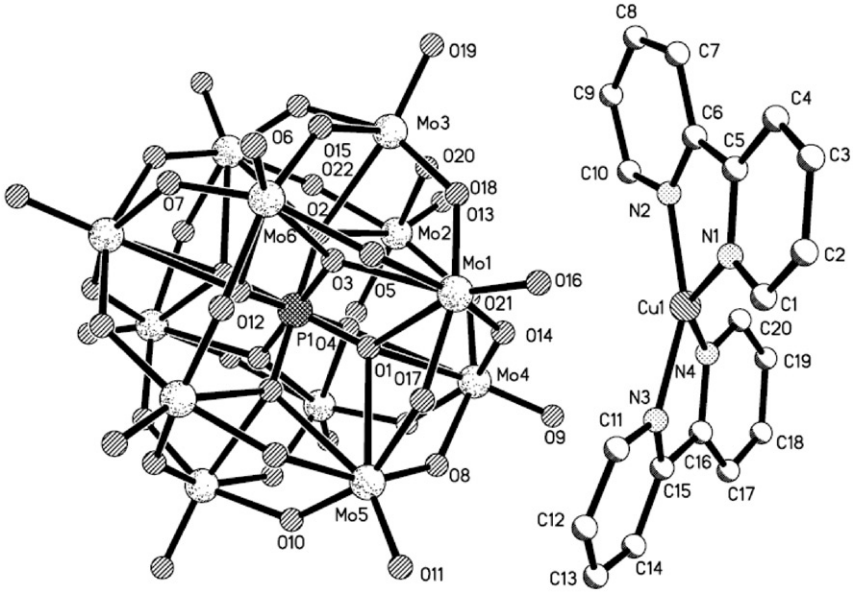

Figure 3. Molecular drawing of **2** showing the labeling of atoms; all H atoms and the solvent water molecule are omitted for clarity.

and 2.871 Å are slightly larger than corresponding values in **1** (2.560 and 2.864 Å). In addition, there are extensive hydrogen bonds among the water molecules (O2w and O3w) and the $[Mo^{V}Mo^{VI}_{11}O_{36}(PO_4)]^{4-}$ cluster in **2**, with $O22\cdots O2w$ of 1.970 Å, $O9\cdots O1w$ of 2.850 Å, $O17^{\#}\cdots O2w$ of 1.949 Å, $O5^{\#}\cdots O2w$ of 1.958 Å and $O12^{\#}\cdots O2w$ of 2.003 Å (# is a symmetry code). These weak interactions also play important roles in stabilization of the molecule in the crystal structure of **2**.

The assignment of the oxidation states for the Mo atoms is in agreement with the electric charge and bond valence sum calculations [14]. Calculation based on the equation $S = \exp[1-(R-R_0)/B]$, the valence sums for twelve Mo atoms are Mo1(2×): 6.030, Mo2(2×): 5.974, Mo3(2×): 5.834, Mo4(2×): 5.922, Mo5(2×): 5.806 and Mo6(2×): 6.094, the average value of which is 5.94 (the expected average value for $Mo^{V}Mo^{VI}_{11}$ is 5.92). The calculated results indicate only one Mo center is in the +5 oxidation state with one delocalized electron.

3.3. *Magnetic properties*

The magnetic susceptibilities of **2** were measured in the 2–300 K temperature range and shown as χT and $1/\chi$ *versus* T plots in figure 5. At room temperature, the χT value of 1.11 emu K mol^{-1} is a little smaller than expected for the total spin-only value of two isolated spin-only $S = 1/2$ spins of Cu^{2+} atoms and 1 uncoupled $S = 1/2$ spin of Mo^{5+} atom ($\approx$1.125 emu K mol^{-1} supposing $g = 2.0$ for Cu^{2+} and Mo^{5+}). The χT value continuously increases with deceasing temperature down to 8 K, suggesting the presence of ferromagnetic exchange interactions. The temperature dependence of $1/\chi$ in the range of 100–300 K is in good agreement with the Curie–Weiss law with $C = 0.99$ emu K mol^{-1} and $\Theta = -31.9$ K. The positive Weiss constant confirms the

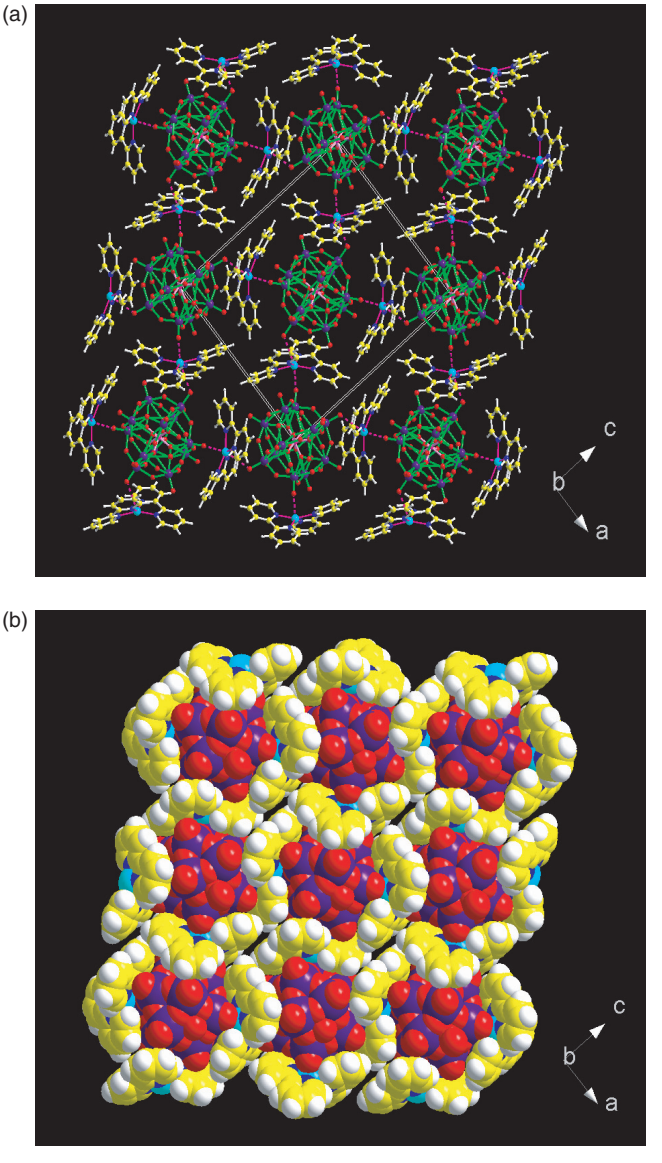

Figure 4. (a) A view of the 2D layer 12-polymolybdate-based inorganic metal-organic hybrid supramolecular network of **2** maintained by Cu···$O_{polyoxoanion}$ short contact weak interactions, all H atoms are omitted for clarity. (b) Space-filling model for **2**.

presence of ferromagnetic exchange interaction between adjacent Cu(II) and Mo(IV) ions, which is obviously mediated by Cu···$O_{polyoxoanion}$ short contact weak interaction between the reduced 12-molybdophosphate anion $[Mo^{V}Mo^{VI}_{11}O_{36}(PO_4)]^{4-}$ and $[Cu(2,2'\text{-bpy})_2]^{2+}$. At 8 K, the χT value reaches a maximum of 1.63 emu K mol^{-1} and then decreases below this temperature probably owing to saturation of the χ value. No magnetic order or spin glass behavior was observed by ZFC-FC and AC determinations.

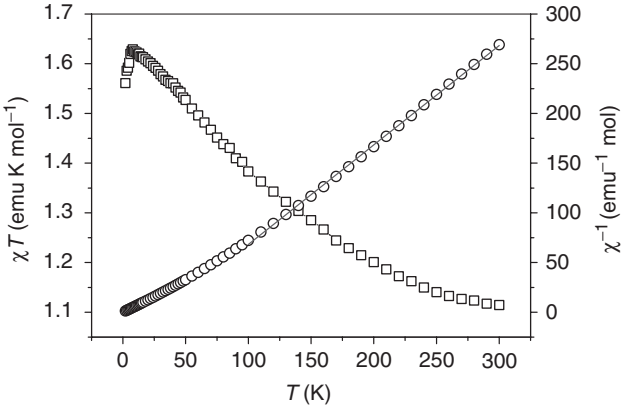

Figure 5. Plots of $\chi_M T$ and χ_M *vs.* T of **2**.

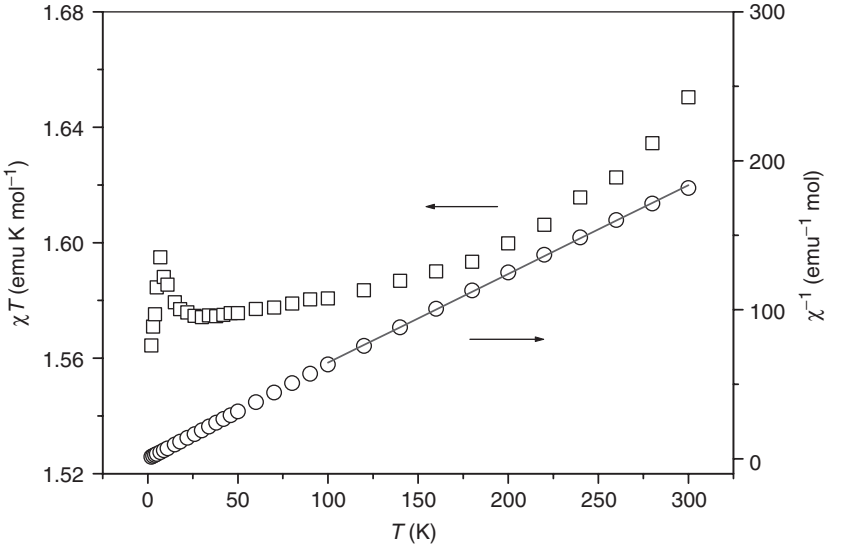

Figure 6. Plots of $\chi_M T$ and χ_M *vs.* T of **1**.

Magnetic susceptibility data for complex **1** over the temperature range 2–300 K are shown in figure 6. The observed χT value of 1.65 emu K mol^{-1} at 300 K is much smaller than the expected value of 3.375 emu K mol^{-1} for two non-interacting $S = 1/2$ Cu^{2+} cations, two isolated spin-only $S = 1/2$ V^{4+} cations and five uncoupled $S = 1/2$ Mo^{4+} cations (assuming $g = 2$ for Cu^{2+}, V^{4+} and Mo^{5+}) (figure 6). Upon cooling, χT value slightly deceases and reaches a minimum of 1.57 emu K mol^{-1} at 30 K, indicating an antiferromagnetic interaction. This is confirmed by a negative Weiss constant (−2.9 K) determined in the temperature range 100–300 K. Such an antiferromagnetic coupling is attributed to electron delocalization in the reduced mixed-valence polyoxoanion [3j, 3l, 4f, 15]. The increase of χT below 30 K could be due to a contribution from ferromagnetic coupling, which is obviously dominant at low temperature. The origin of such a ferromagnetic exchange is to the $Cu \cdots O_{polyoxoanion}$ short contact weak

interaction between the polyoxoanion $[V^{IV}{}_2Mo^{V}{}_5Mo^{VI}{}_7O_{38}(PO_4)]^{4-}$ and the complex fragment cation $[Cu(2,2'\text{-bpy})_2]^{2+}$, which may mediate the ferromagnetic coupling as in **2**. At 7 K, the χT value reaches a maximum of 1.59 emu K mol^{-1} and then decreases below this temperature probably due to saturation of the χ value. Unfortunately, it is difficult to fit the experimental magnetic data in the overall range for **1** and **2** using suitable theoretical models [16], no further magnetic analysis is supplied at present.

4. Conclusion

In summary, hydrothermal reactions of NH_4VO_3, $H_3[P(Mo_3O_{10})_4]\cdot xH_2O$ and suitable Cu^{2+} salts in the presence of 2,2′-bipy ligand yielded two 2D layer polyoxometalate-based inorganic metal-organic hybrid supramolecular complexes $[Cu(2,2'\text{-bpy})_2]_2[V^{IV}{}_2Mo^{V}{}_5Mo^{VI}{}_7O_{38}(PO_4)]$ (**1**) and $[Cu(2,2'\text{-bpy})_2]_2[Mo^{V}Mo^{VI}{}_{11}O_{36}(PO_4)]\cdot 3H_2O$ (**2**). Inter-molecular $Cu\cdots O_{polyoxoanion}$ short contact weak interactions connect polyoxoanions and complex fragment cations $[Cu(2,2'\text{-bpy})_2]^{2+}$ in both complexes, and mediate ferromagnetic interactions. This work provides examples of short contact weak interaction in guiding self-assembly of high-dimensional polyoxometalate-based inorganic metal-organic hybrid supramolecular complexes, demonstrating that non-covalent short contact weak interactions between the terminal oxygen atom in polyoxoanions and the transition metal center in complex fragment cations can be utilized in place of a classic covalent bond to build high dimensional polyoxometalate-based inorganic metal-organic hybrid supramolecular networks; metal$\cdots$anion short contact weak interaction can play an important role in crystal engineering for construction of supramolecular complexes.

Supplementary material

Crystallographic data have been deposited with the Cambridge Crystallographic Data Center with the CCDC reference numbers 296083 and 296084. Copies of this information may be obtained free of charge free from The Director, CCDC, 12 Union Road, Cambridge, CB2 1EZ, UK (Fax: t44-1223-336033; Email: deposit@ccdc.cam.ac.uk).

Acknowledgements

This work was supported by National Natural Science Foundation of China (Nos. 20201012, 20473096, 90101025), the Major State Basic Research Development Program of P.R. China (2001CB610507) and Chinese Academy of Sciences.

References

[1] (a) D. Braga, L. Brammer, N.R. Champness. *Cryst. Eng. Comm.*, **7**, 650 (2005); (b) G.R. Desiraju. *Acc. Chem. Res.*, **35**, 565 (2002); (c) G.R. Desiraju. *Chem. Commun.*, 1475 (1997).

[2] (a) E. Coronado, C.J. Gómez-García. *Chem. Rev.*, **98**, 273 (1998); (b) P.J. Hagrman, D. Hagrman, J. Zubieta. *Angew. Chem. Int. Ed.*, **38**, 2638 (1999); (c) G. Centi, F. Trifro, J.R. Ebbner, V.M. Franchetti. *Chem. Rev.*, **88**, 55 (1988); (d) D. Braga, F. Grepioni, G.R. Desiraju. *Chem. Rev.*, **98**, 1375 (1998).

[3] For examples: (a) A. Müller, M. Koop, P. Schiffels, H. Bögge. *Chem. Commun.*, 1715 (1997); (b) R.S. Rarig Jr., L. Bewley, V. Golub, C.J. O'Connor, J. Zubieta. *Inorg. Chem. Commun.*, **6**, 539 (2003); (c) V. Shivaiah, S.K. Das. *Inorg. Chem.*, **44**, 8846 (2005); (d) J.-Q. Xu, R.-Z. Wang, G.-Y. Yang, Y.-H. Xing, D.-M. Li, W.-M. Bu, L. Ye, Y.-G. Fan, G.-D. Yang, Y. Xing, Y.-H. Lin, H.-Q. Jia. *Chem. Commun.*, 983 (1999); (e) Y. Xu, J.-Q. Xu, K.-L. Zhang, Y. Zhang, X.-Z. You. *Chem. Commun.*, 153 (2000); (f) W. Yang, C. Lu, H. Zhuang. *J. Chem. Soc., Dalton Trans.*, 2879 (2002); (g) G. Luan, Y. Li, S. Wang, E. Wang, Z. Han, C. Hu, N. Hu, H. Jia. *J. Chem. Soc., Dalton Trans.*, 233 (2003); (h) M. Yuan, Y. Li, E. Wang, C. Tian, L. Wang, C. Hu, N. Hu, H. Jia. *Inorg. Chem.*, **42**, 3670 (2003); (i) C.-L. Pan, J.-Q. Xu, Y. Sun, D.-Q. Chu, L. Ye, Z.-L. Lü, T.-G. Wang. *Inorg. Chem. Commun.*, **6**, 233 (2003); (j) C.-M. Liu, S. Gao, H.-M. Hu, Z.-M. Wang. *Chem. Commun.*, 1636 (2001); (k) C.-M. Liu, D.-Q. Zhang, D.-B. Zhu. *Cryst Growth & Des.*, **3**, 363 (2003); (l) C.-M. Liu, Y.-H. Huang, D.-Q. Zhang, F.-C. Jiang, D.-B. Zhu. *J. Coord. Chem.*, **56**, 953 (2003); (m) C.-M. Liu, D.-Q. Zhang, C.-Y. Xu, D.-B. Zhu. *Solid State Sci.*, 689 (2004).

[4] For examples: (a) D. Hagrman, C. Zubieta, D.J. Rose, J. Zubieta, R.C. Haushalter. *Angew. Chem. Int. Ed.*, **36**, 873 (1997); (b) P.J. Zapf, C.J. Warren, R.C. Haushalter, J. Zubieta. *Chem. Commun.*, 1543 (1997); (c) W.-M. Bu, L. Ye, G.-Y. Yang, J.-S. Gao, Y.-G. Fan, M.-C. Shao, J.-Q. Xu. *Inorg. Chem. Commun.*, **4**, 1 (2001); (d) C.-D. Wu, C.-Z. Lu, H.-H. Zhuang, J.-S. Huang. *Inorg. Chem.*, **41**, 5636 (2002); (e) C.-Z. Lu, C.-D. Wu, H.-H. Zhuang, J.-S. Huang. *Chem. Mater.*, **14**, 2649 (2002); (f) C.-M. Liu, J.-L. Luo, D.-Q. Zhang, N.-L. Wang, Z.-J. Chen, D.-B. Zhu. *Eur. J. Inorg. Chem.*, 4774 (2004); (g) C.-M. Liu, D.-Q. Zhang, D.-B. Zhu. *Cryst. Growth & Des.*, **5**, 1639 (2005); (h) J. Luo, M. Hong, R. Wang, Q. Shi, R. Cao, J. Weng, R. Sun, H. Zhang. *Inorg. Chem. Commun.*, **6**, 702 (2003); (i) C.-M. Liu, D.-Q. Zhang, D.-B. Zhu. *Cryst Growth & Des.*, **6**, 524 (2006); (j) J.-Y. Niu, D.-J. Guo, J.-P. Wang, J.-W. Zhao. *Cryst. Growth & Des.*, **4**, 241 (2004).

[5] For examples: (a) D. Hagrman, P.J. Zapf, J. Zubieta. *Chem. Commun.*, 1283 (1998); (b) R.L. LaDuca, Jr. R. Finn, J. Zubieta. *Chem. Commun.*, 1669 (1999); (c) D. Hagrman, P.J. Hagrman, J. Zubieta. *Inorg. Chem. Acta*, **300–302**, 212 (2000); (d) R.C. Finn, J. Zubieta. *Inorg. Chem.*, **40**, 2466 (2001); (e) B. Yan, Y. Xu, X. Bu, N.K. Goh, L.S. Chia, G.D. Stucky. *J. Chem. Soc., Dalton Trans.*, 2009 (2001); (f) B E. urkholder, J. Zubieta. *Chem. Commun.*, 2056 (2001); (g) S. Reinoso, P. Vitoria, L.S. Felices, L. Lezama, J.M. Gutiérrez-Zorrilla. *Inorg. Chem.*, **45**, 108 (2006); (h) J. Chen, S. Lu, R.Yu, Z. Chen, Z. Huang, C. Lu. *Chem. Commun.*, 2640 (2002); (i) L. Zhang, X. Zhao, J. Xu, T. Wang. *J. Chem. Soc., Dalton Trans.*, 3275 (2002); (j) L.-M. Duan, C.-L. Pan, J.-Q. Xu, X.-B. Cui, F.-T. Xie, T.-G. Wang. *Eur. J. Inorg. Chem.*, **14**, 2578 (2003);. (k) Y. Lu, Y. Xu, E. Wang, J. Lü, C. Hu, L. Xu. *Cryst Growth & Des.*, **5**, 257 (2005); (l) C.-M. Liu, D.-Q. Zhang, M. Xiong, D.-B. Zhu. *Chem. Commun.*, 1416 (2002).

[6] (a) D. Hagrman, J. Zubieta. *Chem. Commun.*, 2005 (1998); (b) B.Z. Lin, S.-X. Liu. *Chem. Commun.*, 2126 (2002); (c) Y. Lu, Y. Li, E. Wang, J. Lü, L. Xu, R. Clérac. *Eur. J. Inorg. Chem.*, 1239 (2005).

[7] For examples: (a) *Crystal Design Structure and Function, Perspectives in Supramolecular Chemistry*, G.R. Desiraju (Ed.), Vol. 7, John Wiley & Sons, Ltd. (2003). (b) J.C. MacDonald, G.M. Whitesides. *Chem. Rev.*, **94**, 2383 (1994); (c) H.W. Roeskya, M. Andruh. *Coord. Chem. Rev.*, **236**, 91 (2003); (d) B. Moulton, M.J. Zaworotko. *Chem. Rev.*, **101**, 1629 (2001); (e) G.R. Desiraju. In *Stimulating Concepts in Chemistry*, F. Vögtle, J.F. Stoddart, M. Shibasaki (Eds), p. 293, Wiley; VCH, Weinheim (2000). (f) C. Janiak. *J. Chem. Soc. Dalton Trans.*, 3885 (2000).

[8] A.J. Blake, N.R. Champness, P. Hubberstey, W.-S. Li, M.A. Withersby, M. Schröder. *Coord. Chem. Rev.*, **183**, 117 (1999).

[9] M.A. Withersby, A.J. Blake, N.R. Champness, P. Hubberstey, W.-S. Li, M. Schröder. *Angew. Chem. Int. Ed.*, **36**, 2327 (1997).

[10] (a) P.-Q. Zheng, Y.-P. Ren, L.-S. Long, R.-B. Huang, L.-S. Zheng. *Inorg. Chem.*, **44**, 1190 (2005). (b) X.-M. Zhang, X.-M. Chen. *Inorg. Chem. Commun.*, **6**, 206 (2003).

[11] Q. Chen, C.L. Hill. *Inorg. Chem.*, **35**, 2403 (1996).

[12] (a) H. Nakai. *Bull. Chem. Soc. Jpn.*, **44**, 2412 (1971); (b) H. Nakai. *Bull. Chem. Soc. Jpn.*, **56**, 1637 (1983); (c) J. Foley, S. Tyagi, B.J. Hathaway. *J. Chem. Soc., Dalton Trans.*, 1 (1984).

[13] C.-M. Liu, R.-G. Xiong, X.-Z. You, Y.-J. Liu, K.-K. Cheung. *Polyhedron*, **15**, 4565 (1996).

[14] (a) M. O'Keeffe, N.E. Brese. *J. Am. Chem. Soc.*, **113**, 3226 (1991); (b) M. O'Keeffe, A. Navrotsky (Ed). *Structure and Bonding in Crystals*, Vol. II, p. 1, Academic Press, New York (1981).

[15] (a) D. Gatteschi, L. Pardi, A.L. Barra, A. Müller, J. Döring. *Nature*, **354**, 463 (1991); (b) A.-L. Barra, D. Gatteschi, L. Pardi, A.L. Barra, A. Müller, J. Döring. *J. Am. Chem. Soc.*, **114**, 8509 (1992); (c) A. Müller, R. Sessoli, E. Krickemeyer, H. Bögge, J. Meyer, D. Gatteschi, L. Pardi, J. Westphal, K. Hovermeier, R. Rohlfing, J. Döring, F. Hellweg, C. Beugholt, M. Schmidtmann. *Inorg. Chem.*, **36**, 5239 (1997); (d) T. Yamase, H. Makino, H. Naruke, A.M.S.J. Wéry. *Chem. Lett.*, 1350 (2000).
[16] O. Kahn. *Molecular Magnetism*, VCH, Weinheim, Germany (1993).